

Molecular dynamics simulations of the graphene sheet aggregation in dodecane

Shenghui Chen · Shuangqing Sun · Chunling Li ·
Charles U. Pittman Jr · Thomas E. Lacy ·
Songqing Hu · Steven R. Gwaltney

Received: 22 March 2017 / Accepted: 11 May 2017 / Published online: 1 June 2017
© Springer Science+Business Media Dordrecht 2017

Abstract Molecular dynamics simulations are used to investigate the aggregation and behavior of two parallel graphene sheets (22.0–64.0 Å in length) in dodecane. The dodecane layer formed on the graphene surface leads to an energy barrier which slows the rate of the graphene aggregation process when the two sheets are totally separated by dodecane molecules. The graphene sheets aggregate in dodecane only when portions of one graphene sheet are in contact with another sheet. The aggregation rate depends on the combined structures of the two graphene sheets. The aggregation rate for two parallel graphene sheets in half contact with one another is constant since the relative sheet geometry and spacing are nearly constant in the transition region between sheets where dodecane molecules are being displaced

during aggregation. The aggregation rate for partially overlapped graphene sheets becomes progressively slower as aggregation continues since the area not overlapped decreases as the aggregation proceeds.

Keywords Graphene sheets · Dodecane · Aggregation · Molecular dynamics · Modeling and simulation · Graphene-based composites

Introduction

Graphene has attracted significant attention due to its superior properties (Novoselov et al. 2004; Geim and Novoselov 2007; Lee et al. 2008; Zhu et al. 2010; Sadasivuni et al. 2014). At the same time, graphene-based composites have shown unique properties and improved mechanical, thermal, gas barrier, and electrical properties (Eda and Chhowalla 2009; Kuilla et al. 2010; Singh et al. 2011; Huang et al. 2012). Graphene reinforcements improved the fracture and fatigue resistance of an epoxy polymer to the same degree as carbon nanotube (CNT) reinforcements, but the graphene weight fraction to achieve this was one to two orders of magnitude lower than that of the CNTs (Rafiee et al. 2010). Graphene improved mechanical and electrical properties much more than clay or other carbon fillers in polymer composites (Eda and Chhowalla 2009; Kuilla et al. 2010; Singh et al. 2011; Huang et al. 2012). These unusual properties make graphene-based composites attractive for a wide range of potential

S. Chen · S. Sun (✉) · C. Li · S. Hu (✉)
College of Science, China University of Petroleum,
Qingdao 266580, People's Republic of China
e-mail: sunshuangqing@upc.edu.cn
e-mail: songqinghu@upc.edu.cn

C. U. Pittman Jr, · S. R. Gwaltney
Department of Chemistry, Mississippi State University,
Mississippi State, MS 39762, USA

T. E. Lacy
Department of Aerospace Engineering, Mississippi State
University, Mississippi State, MS 39762, USA

S. Hu
Key Laboratory of New Energy Physics & Materials Science,
Universities of Shandong (China University of Petroleum),
Qingdao 266580, China

applications (Hu et al. 2014; Mittal et al. 2015; Tien and Teng 2010).

Unfortunately, like other nanomaterials with high aspect ratios, graphene sheets tend to irreversibly agglomerate, or even restack to form graphite, if the sheets are not well separated from each other. This results from strong intersheet van der Waals forces and π - π interactions (Si and Samulski 2008a, 2008b). The reported cleavage energy of graphite was about 61 meV/atom (Zacharia et al. 2004). Such strong sheet attractions make it difficult to form uniform and homogeneous dispersions into a host matrix. As a result, the aggregated graphene sheets behave no differently than graphite platelets, and the improvement of composite properties is reduced. The aggregation deleteriously affects the applications of graphene-based composites. Thus, studies of the aggregation process and microbehavior of graphene sheets in the host matrix have great significance.

Recently, many experiments to reduce the aggregation were conducted (Stankovich et al. 2006; Wei et al. 2009; Li et al. 2008; Yang et al. 2011). However, many facets of aggregation and the behavior of graphene sheets in a liquid resin are still unknown. Experimental studies of graphene sheet aggregation at the nanometer level are very difficult. Molecular dynamics (MD) modeling offers a means to probe the behavior of graphene sheets, and many MD simulation studies about graphene-based composites have been published (Zhang et al. 2012). Lv et al. (2010) investigated the influence of the chemical functionalization of graphene on the interfacial bonding characteristics between graphene and polymers using MD simulations. Zhang and Jiang (2014) elucidated the structural and mechanical properties of graphene/graphene oxide paper and their polymer composites using MD simulations. Shokrieh et al. (2014) combined MD simulations and micromechanics methods to predict graphene/epoxy nanocomposite moduli, obtaining good agreement with experimental data. Nouranian et al. (2011) and Jang et al. (2012, 2013) studied the interphase between a vinyl ester resin and graphene sheet surfaces in composites, and the interfacial adhesion between graphite nanoplatelets and a vinyl ester polyester matrix was also studied using MD simulations. To date, most graphene composite simulations have focused on predicting composite properties and the interactions between graphene and matrix molecules. MD simulations have proved to be a useful tool to study graphene-based composites. But MD simulations of

graphene aggregation and the microbehaviors of graphene sheets in a host matrix are scarce.

In the present work, MD simulations followed the aggregation of graphene sheets in dodecane. Dodecane was selected as a standard linear hydrocarbon nonpolar solvent, representative of kerosene, petroleum ether, gasoline, etc. It will interact with graphene differently than branched alkanes, which are unable to orient on the surface of graphene the same way as linear dodecane. The results obtained with dodecane would be interesting to eventually compare to those of a highly branched C-12 alkane as well as results from aromatic nonpolar and other more polar solvents. Three model structures were built: (1) parallel graphene structures with and without dodecane between them; (2) a half-contact graphene structure where dodecane is present in between two sheets over half their area, and in the other half, these two sheets are in contact; and (3) overlapped graphene structures, where a portion of two sheets are overlapped, either with or without dodecane present between the sheets in this overlapped region. The aggregation behaviors of dodecane-separated and contacted graphene sheets are investigated at the nanometer level. This work improves the understanding of unoxidized graphene aggregation and stacking in dodecane, a nonpolar saturated hydrocarbon.

Calculation models and methods

All simulations were performed using Materials Studio software (Accelrys Inc.). The Condensed-Phase Optimized Molecular Potentials for Atomistic Simulation Studies (COMPASS) force field developed by Sun (1998) was used in this work. It is a commonly used, well-calibrated hydrocarbon force field (Wu et al. 2016; Arash et al. 2014; Zheng et al. 2007; Asche et al. 2016). It has previously been successfully employed in simulations of graphene sheets in liquid resins and composites (Lv et al. 2010; Zhang and Jiang 2014; Nouranian et al. 2011; Jang et al. 2012; Jang et al. 2013; Chen et al. 2016). In this study, the van der Waals and pi-pi interactions between graphene sheets play an important role in the graphene aggregation. The COMPASS force field contains a Lennard-Jones 9-6 term for the van der Waals interactions. Paton and Goodman (2009) showed that such term could describe van der Waals and pi-pi interactions quite reasonably. However, pi-pi stacking is not a well-defined concept, and the field of intermolecular

interactions would be better off to stop using it (Martinez and Iverson 2012). What is usually thought of as pi-pi stacking is really a combination of normal VdW interactions and solvent-solute interactions, which are all included in our simulations. In recent years, the COMPASS force field has been commonly used in similar simulations, which included VdW and pi-pi interactions of graphene in the models (Fouquet et al. 2009; Pan et al. 2007; Shao et al. 2012; Jiang et al. 2011; Li et al. 2011). The Ewald method for the Coulomb interaction and the atom-based method for the van der Waals interaction, with a 12.5-Å cutoff distance, were selected. All MD simulations were run using the constant number of particles, volume, and temperature (NVT) ensemble.

In order to study graphene sheet aggregation, a model medium of dodecane molecules containing two graphene sheets was built. There are a huge number of possible combinations for the two sheets. In this work, the parallel, half-contact, and lapped graphene structures mentioned previously were selected for simulation.

Parallel graphene structure and calculation methods

This simple parallel structure contains two graphene sheets (sheet 1 and sheet 2) parallel to each other (Fig. 1). Sheet 1 is a continuous graphene sheet lying in the xy plane, while sheet 2 has finite width in the x -direction and is continuous in the y -direction, in order to allow the dodecane molecules to diffuse into or out from the intersheet spacing between the sheets. Two models (model A and model B) were constructed with different intersheet distances as initial structures. In model A, the graphene sheets are initially in direct contact with each other with no dodecane molecules between them, and the distance between the two sheets was 3.4 Å. The distance between the two sheets was 6.8 Å in model B, and the two graphene sheets are already separated by dodecane molecules. To simplify the simulations, all the atoms of sheet 1 are fixed in these two models, and all other atoms are allowed to relax.

The cell size is $41.8 \times 51.1 \times 45.0 \text{ \AA}^3$ for both models A and B (Fig. 1). The length of sheet 2 is 22.0 Å in the x -direction. A geometry optimization was carried out for 10,000 iterations using the smart minimizer method to minimize the total energy before MD simulations. A previously described, the annealing MD simulation method (Nouranian et al. 2011; Jang et al. 2012; Zhao and Hu 2013) was used to accelerate the calculations. First, the MD simulation was run for 2 ps at 10 K. Then,

the temperature was increased to 50 K and then further raised to 1000 K in increments of 50 K. At each intermediate temperature, the dynamics simulation was run for 2 ps. A 4-ns dynamics simulation was run at 1000 K to obtain an equilibrated structure. After that, the cell was cooled to 300 K in 50-K decrements, with 2-ps MD simulations completed at the intermediate temperatures. Then, the MD simulation was continued for another 4 ns at 300 K to ensure structure equilibration. All of the analyses described for these two models were obtained from the last 1 ns of the MD simulations at 300 K. The same procedure was used for both systems. One snapshot every 10 ps was used for the analyses.

Half-contact graphene structure and calculation methods

The half-contact graphene structure is shown in Fig. 2. This model (model C) also contains two graphene sheets (sheet 1 and sheet 2). Both sheets are continuous in the y -direction, while discontinuous in the x -direction. In the x -direction, the length of sheet 1 is 64.0 Å, while sheet 2 is a little shorter, 62.2 Å. Half of sheet 2 is in direct contact with sheet 1 with a 3.4-Å distance between the two sheets. The length of the direct contacted area is 29.4 Å. The left half of sheet 2 is separated from sheet 1 by intercalated dodecane molecules with a 7.7-Å distance between the two sheets.

The model C cell size is $91.0 \times 38.3 \times 40 \text{ \AA}^3$ (Fig. 2). Before simulating the aggregation of the two sheets, a MD annealing simulation was performed with the two graphene sheets fixed to make sure all dodecane molecules are fully relaxed. This annealing simulation was the same as that described in [Parallel graphene structure and calculation methods](#). After annealing was completed, all the atoms, including the atoms of the two graphene sheets, were relaxed to simulate a real aggregation process. This aggregation MD simulation for model C was run for 25 ns at 300 K. This long simulation was employed because the two-sheet aggregation in model C was much slower than the other models. This 25-ns MD simulation was analyzed to investigate the aggregation process.

Overlapped graphene structure and calculation methods

Figure 3 shows the two overlapped graphene models (models D and E). In these two models, both graphene sheets are parallel to each other, and both are discontinuous in the x -direction. The two sheets are not completely

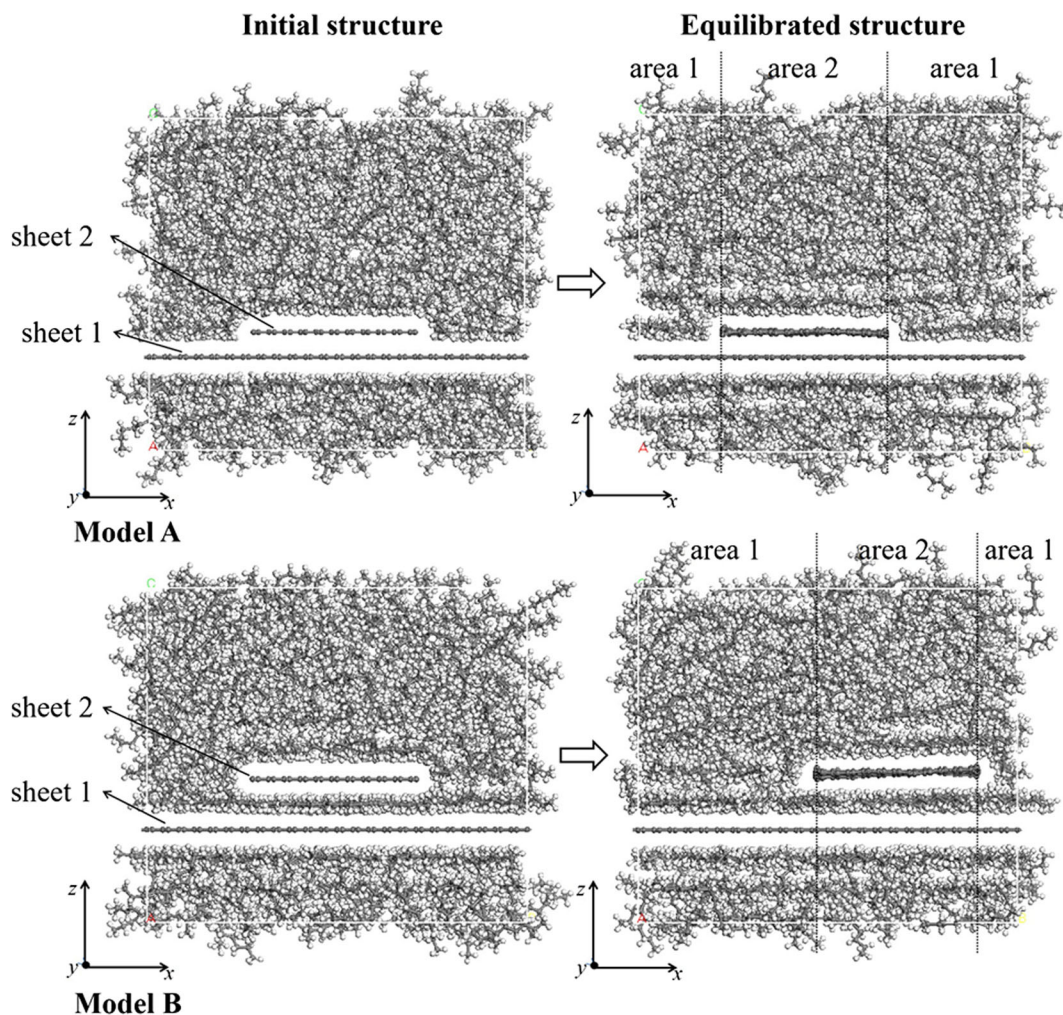


Fig. 1 Initial structures and equilibrated structures of the parallel graphene models (models A and B)

overlapped. Only one end from each sheet is overlapped. In both models D and E, the length of this overlapped region in the x -direction is 7.4 \AA . The length of the two sheets is 35.7 \AA in the x -direction. In model D, the distance between the two sheets is 3.4 \AA with no dodecane present in the interlayer spacing. In contrast, for model E, dodecane molecules separate the two overlapped sheets, with 6.8 \AA distance between the two sheets.

The cell size for both models D and E is $91.0 \times 38.3 \times 40 \text{ \AA}^3$ (Fig. 3). Similar to the procedure used with model C (half-contact graphene structure), the MD annealing simulation was conducted where the two graphene sheets were fixed to allow the dodecane molecules to fully relax. Also, the MD full annealing simulation was the same. After completing the annealing simulation, the atoms of the two sheets were relaxed to

allow them to move freely. Then another 11 ns simulation was run at 300 K to simulate the real aggregation of the two sheets. All results concerning these overlapped graphene models were obtained from this 11 ns simulation.

Results and discussion

Parallel graphene structures of models A and B

Resulting structures

The equilibrated structures of models A and B are shown in Fig. 1. In model A, the graphene sheets are still in contact and no dodecane molecules penetrated

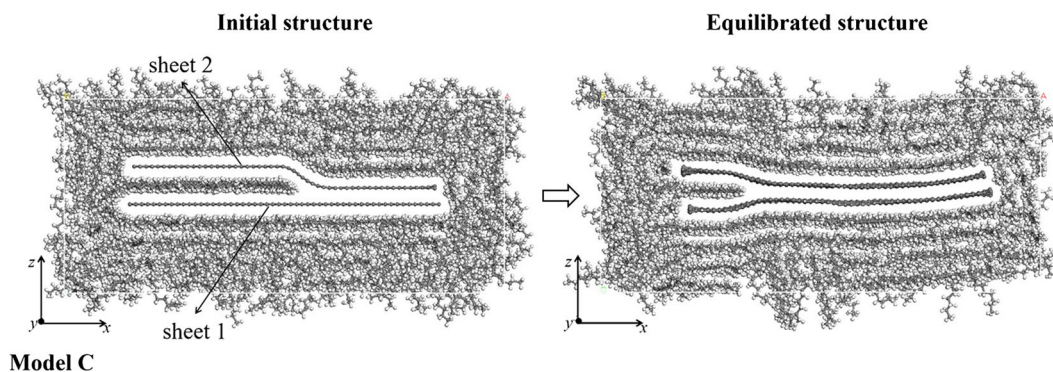


Fig. 2 Initial structure and equilibrated structure of half-contact graphene model (model C). Length of graphene sheets, 64.0 Å

into the interlayer spacing when the initial distance between sheets is 3.4 Å. However, when the initial distance between sheets is 6.8 Å, the graphene sheets never get close enough to aggregate but stay separated with dodecane molecules remaining between the two sheets, with a distance similar to the initial interlayer distance.

Structure of the graphene sheets in models A and B

After equilibration, sheet 2 is almost perpendicular to the z -axis (Fig. 1). The average z -coordinates of the atoms in sheet 2 are used to indicate sheet 2's position

in the z -direction. Thus, the distance between sheets 1 and 2 is calculated from the differences of the average z -coordinates for the two sheets. Figure 4 shows the interlayer distances for the two models during the last 1 ns MD simulation, where these distances remain stable for both models A and B.

In model A, the interlayer distance between sheets is stable at 3.4 Å (Fig. 4), which is the same as the d -spacing of graphite. Sheet 2 does not move in the z -direction during the equilibration. The strong attractive interaction between the two graphene sheets keeps them in contact, hindering dodecane from diffusing into the interlayer spacing over the entire simulation. In contrast,

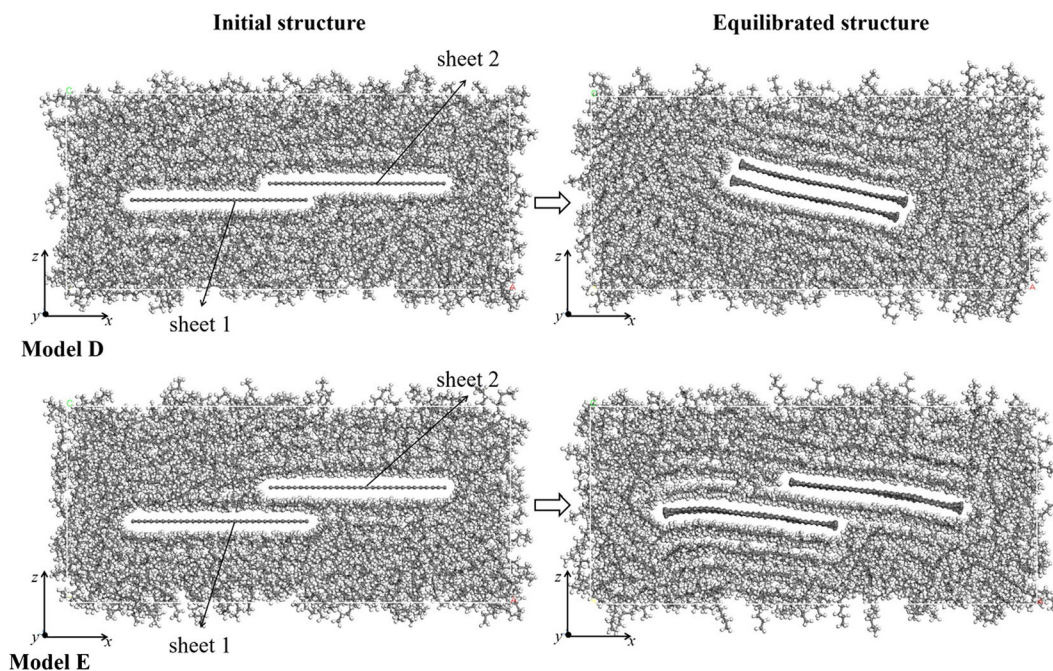


Fig. 3 Initial structures and equilibrated structures of the lapped graphene models (model D and E). Length of graphene sheets, 35.7 Å

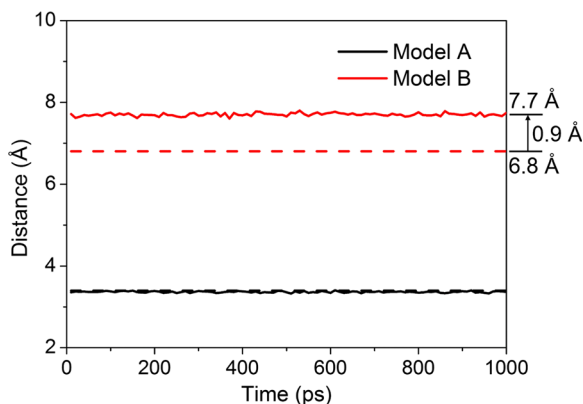


Fig. 4 Interlayer distance in the initial and equilibrated structures for models A and B. The *dashed lines* represent the interlayer distance in the *initial* structures, and the *solid lines* are for the *equilibrated* structures

the distance between the two sheets in model B increases to 7.7 Å, from its initial distance of 6.8 Å. The dodecane molecules remain in the interlayer spacing. The interaction between the two graphene sheets at a 6.8-Å separation distance cannot force dodecane out from between the sheets. Dodecane has attractive interactions to the graphene sheet surfaces which contribute to stabilizing of the intersheet spacing on the 8-ns time scale. During the equilibration, some dodecane molecules are observed to diffuse into and out of this interlayer spacing.

In both models A and B, the distance between the two sheets oscillates around the equilibrium position. The two sheets in each equilibrated model do not translate into each other at temperatures under 300 K. An energy barrier between these two equilibrium structures exists, slowing translation. Separating contacted graphene sheets requires overcoming the strong sheet-sheet interaction. Removal of dodecane between separated and parallel graphene sheets must surmount an energy barrier caused by dodecane and graphene interactions. In this simulation (~4 ns at 1000 K and ~4 ns at 300 K), these two equilibrium structures do not interconvert within these time periods. Far longer simulation times would be required to investigate this process, which are well beyond practical limitations. Clearly, this energy barrier greatly slows the graphene aggregation process. Zhao and Hu (2013) simulated graphene dispersion in ionic liquids (ILs) based on the VDW interaction model. Barriers were found due to the formation of metastable states when graphene plates aggregate from large separations to their closest distance in ILs.

Shih et al. (2010) investigated the stabilization mechanism for liquid-phase-exfoliated graphene sheets in polar solvents using molecular dynamics simulations. They also concluded that interactions between graphene and solvent leads to higher energy barriers that hinder the graphene sheet recombination. These results are in accord with our results for dodecane.

Distribution of the dodecane in models A and B

The distribution of dodecane was analyzed by generating the relative concentration profiles in the z -direction for models A and B. The cell was divided into two areas (see Fig. 1): area 1 containing only sheet 1 and area 2 containing sheets 1 and 2. The relative concentration profiles of dodecane carbon atoms in both areas were calculated (Fig. 5 and Fig. 6).

The relative concentration profiles in area 1 in model A (Fig. 5a) are nearly symmetric about graphene sheet 1. Several layers form on both sides of sheet 1. No dodecane is present within the region from 9 to 12 Å since this is the space occupied by sheet 1. In area 2 (Fig. 5b), both sheets occupy this 9- to 15-Å region. Note that the relative concentration profile is relatively symmetric about the two sheets. Moreover, the dodecane relative concentration profile a given distance away from either sheet 1 or sheet 2 in Fig. 5b is consistent with the relative concentration a similar distance from single sheet 1 shown in Fig. 5a. This suggests that the dodecane-dodecane interactions are fairly small across a given graphene sheet and that dodecane-graphene interactions strongly influence the relative concentration profile in the near-sheet region.

In model B, the relative concentration profile of dodecane in area 1 (Fig. 6a) is nearly the same as that found in model A. Several successive dodecane layers form at and are moving away from graphene sheet 1. One dodecane layer forms between the two sheets in area 2 (Fig. 6b). The position of this layer in the z -direction is the same as the position of the first layer in area 1. The thickness and peak relative concentration value of this layer are also similar. Thus, dodecane is adsorbed by the sheets in extended conformations. In return, this layer retards the sheet stacking rate. The new dodecane layers a given distance away from sheet 2 on the sheet 2 side (Fig. 6b) are similar to those a similar distance from single sheet 1 in area 1 (Fig. 6a). Dodecane-graphene interactions strongly influence the

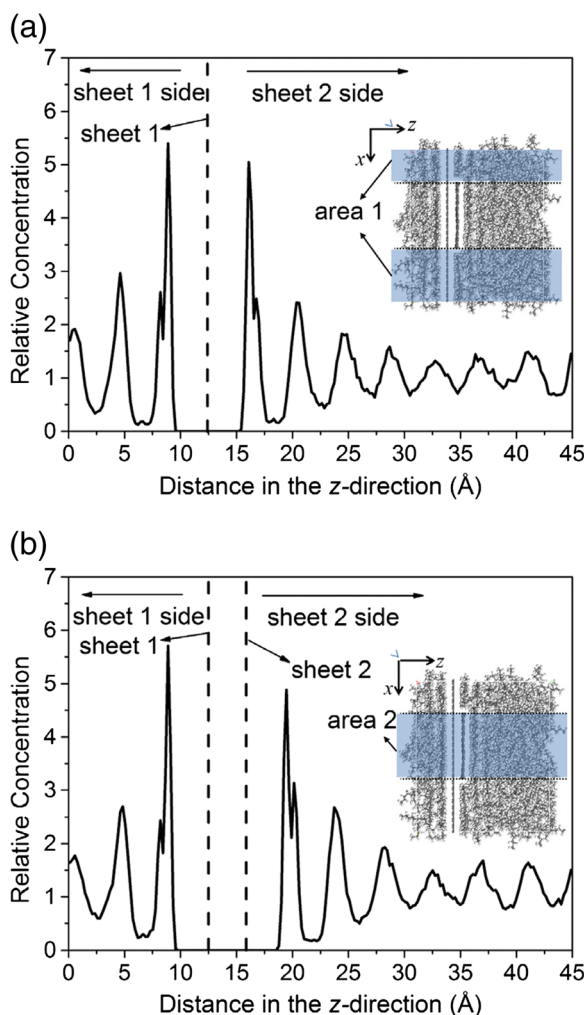


Fig. 5 Relative concentration profiles for the dodecane carbon atoms in the equilibrated model A. **a** For area 1. **b** For area 2

structure of the dodecane matrix. Comparing the difference in the relative concentration profiles in areas 1 and 2 for both models shows that the dodecane distribution can be affected by the number of graphene sheets.

Half-contact graphene structure of model C

Two stacked graphene sheets in full contact cannot be separated by dodecane at 300 K within a 4-ns time frame, and the totally separated graphene sheets in dodecane cannot restack at these same conditions. In this section, graphene sheets in half contact (model C) are simulated (Fig. 2). The sheets are separated by 3.4 Å in the contact area and by 7.7 Å with dodecane present

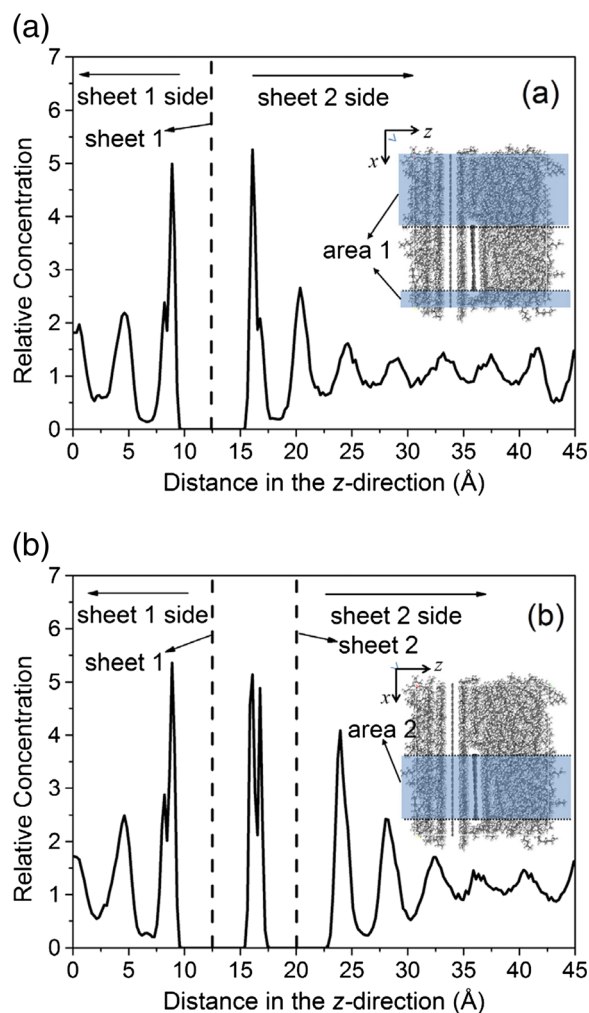


Fig. 6 Relative concentration profiles for carbon atoms of dodecane in the equilibrated model B. **a** For area 1. **b** For area 2

in the uncontacted area (the same situation as equilibrated distance in model B).

Resulting structure of model C

After equilibrating model C for half-contact graphene sheets at 300 K for 25 ns, a larger portion of the sheets have come into contact and a portion of dodecane has diffused out into the bulk solvent (Fig. 2). The length of the remaining dodecane layer between the sheets is much shorter. This illustrates that the half-contact graphene sheets can push out the dodecane molecules between them. However, after even 25 ns MD simulation, some dodecane remains between the two graphene sheets, indicating that the stacking process is still in progress.

Aggregation process in model C

In order to assess the aggregation process for model C (Fig. 2), the total length of the contacted area between the adjacent graphene sheets was determined as a function of time for the first 25 ns (Fig. 7). To illustrate the degree of aggregation, the ratio of the length of the contacted area to the total length is also shown in Fig. 7. The length of the contacted area increases almost linearly with time, suggesting that the rate of stacking is relatively constant ($\sim 0.94 \text{ \AA/ns}$). At 25 ns, about 20% uncontacted area still remains. Assuming a constant aggregation rate, an additional 12 ns would be required to dispel the remaining dodecane and complete the aggregation of the two sheets.

Recall that two parallel graphene sheets sandwiched about a thin dodecane layer will not aggregate (cf., model B, Fig. 1). In contrast, parallel graphene sheets in partial contact (cf., model C, Fig. 2) may tend to stack together. This process is likely driven by mechanisms in the transition region between the graphene sheets in close contact and the domain where the same sheets are separated by dodecane. In this region, the two sheets have a marked change in curvature (Fig. 8). The graphene sheet flexural energy in the transition region may serve as a driving force to displace the dodecane from between the two sheets (i.e., flat graphene sheets in close contact may minimize the total energy of the system). In addition, the adsorption interaction directly between the two graphene sheets in the transition region may be much higher than the domain where the two sheets are separated by a thin dodecane layer; this increased interaction may also contribute to the stacking

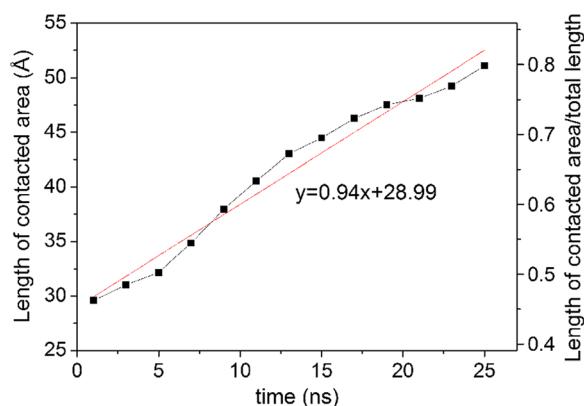


Fig. 7 Length of the contacted area and the ratio of the length of this contacted area to the total length as a function of time for model C

process. As an aside, both the length of the transition region and the geometry of the two sheets in this region remain relatively constant during aggregation; this explains why stacking occurs at a constant rate.

Overlapped graphene structures of models D and E

The proceeding results suggest that (1) the fully contacted graphene sheets in close contact cannot be separated by intercalating dodecane molecules, (2) graphene sheets completely separated by a thin dodecane layer cannot aggregate, and (3) graphene sheets in partial contact will progressively displace any dodecane molecules between them and aggregate. In this section, two overlapped graphene structures are simulated (models D and E), in which only the edges of two graphene sheets are overlapped (Fig. 3).

Resulting structures of models D and E

The resulting equilibrated graphene structures obtained from both idealizations are shown in Fig. 3. In model D, the two partially overlapping graphene sheets with a 3.4-Å initial separation distance translate parallel to their respective planes during equilibration until the edges of each sheet align with the corresponding edge of the other sheet. They finally become completely stacked with each other from an initially partially overlapped

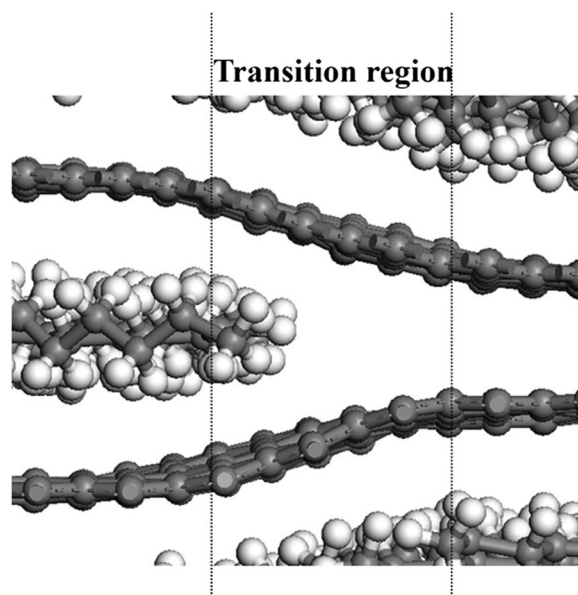


Fig. 8 Transition region between the contacted area and the uncontacted area

geometry. After the MD simulation, no dodecane molecules exist between the two graphene sheets. The dodecane initially adsorbed on the graphene sheets has diffused away from the surface. The distance between the two sheets remains roughly 3.4 Å; this result is consistent with the results obtained for two parallel graphene sheets of unequal length with the same initial separation distance (model A; Fig. 1). When the overlapping graphene sheets are initially separated by 6.4 Å with a corresponding dodecane layer between the sheets (model E; Fig. 3), the relative equilibrium positions of the two sheets are similar to the initial configuration. There are many dodecane molecules residing in the interlayer spacing between these two sheets, and the equilibrium spacing between the sheets in the overlap region is approximately 7.4 Å.

When the overlapped edges of two partially overlapping graphene sheets are initially in close proximity (model D), the strong attraction between the two sheets can displace the adsorbed interlayer dodecane. This leads to realignment (shown in Fig. 3), with eventual graphene stacking. When overlapped sheets are totally separated by dodecane (model E), these parallel graphenes cannot displace the dodecane layer. This is consistent with the results for model B (Fig. 1).

Process of stacking

The realignment/stacking of the partially overlapped graphene sheets was analyzed in model D (3.4 Å initial sheet separation; Fig. 3). The length of the overlapped area in the x -direction was calculated as a function of time (Fig. 9). For comparison purposes, the length of the overlap area was also calculated for the two overlapping sheets sandwiched about a thin dodecane layer (model E; Fig. 3). The ratio of the length of the overlapped area to the total length is shown in Fig. 9 to illustrate the degree of aggregation. In model D, the rate of graphene sheet realignment/stacking was fairly pronounced when the overlapped region was small in comparison to the sheet length (35.7 Å). The rate of stacking decreased progressively until the two graphene sheets were completely stacked.

When two graphene sheets are completely overlapped, no further driving forces exist between the sheets in the direction parallel to the sheet surfaces. However, when two sheets are not fully overlapped while in close proximity, the strong attractions between parallel sheet surfaces provide the driving force to

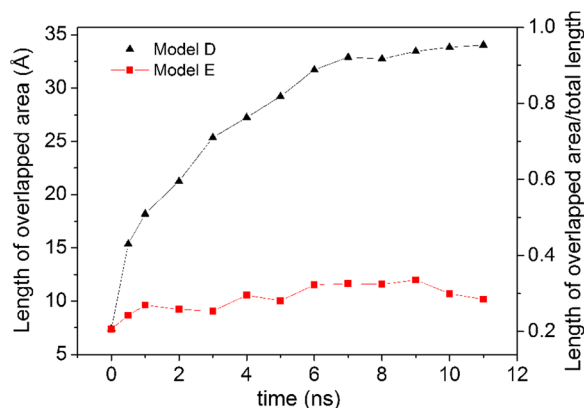


Fig. 9 Length of overlapped area and the ratio of the overlapped area's length as a function of time for models D and E

enlarge the sheet-to-sheet contact area, while displacing dodecane from the surface of the sheet being covered. The graphene sheets can move relative to one another in model D, because the adsorption interactions between the sheets, when moving in the x -direction, is sufficient to displace dodecane at the interface between a given graphene sheet edge and the surface of the adjacent sheet. Since the area that is overlapped is the smallest at the start of the simulation, the sheet motion to gain greater overlap can occur faster. This leads to a faster stacking rate in model D. As the degree of sheet realignment/stacking increases, the existing sheet-to-sheet attractions slow the rate of advancing overlap, decreasing the stacking rate (cf., Fig. 9). Once the length of the overlapped area is 32.9 Å, which occurs at 7 ns, the two sheets are essentially aligned. The rate of alignment between two sheets in the x -direction is too small within the simulation's time scale to drive further observable relative displacement between sheets.

In contrast, the length of the overlapped area for model E changed little throughout the simulation (Fig. 9). The length of the overlapped region ranged between 2.4 and 12.0 Å, with a nominal length of roughly 9.6 Å. Stacking attractions between the two graphene sheets are not sufficient to displace the interstitial dodecane and to drive the alignment near room temperature.

The graphene sheets cannot displace dodecane adsorbed on the graphene surface when the graphene sheets are totally separated by a thin dodecane layer (models B and E). Parallel graphene sheets in partial contact (models C and D) can displace dodecane at the sheet surfaces, leading to sheet aggregation. Two graphene sheets, initially in close contact (model A),

cannot be separated by dodecane. Finally, parallel graphene sheets can aggregate in these simulation time scales, only if part of one graphene sheet is in close contact with another sheet. Parallel graphene sheets cannot aggregate if the two sheets are initially totally separated by dodecane.

Conclusions

In the present work, the aggregation of five different graphene sheet arrangements surrounded by dodecane molecules was investigated using long-time MD simulations. The following conclusions were obtained:

- (1) Near room temperature, parallel graphene sheets aggregate in dodecane only if part (or all) of one graphene sheet is in close contact with the second sheet, with no dodecane molecules present in the contact region. When the two sheets are separated by a thin dodecane layer, the interaction between dodecane and graphene leads to an energy barrier which markedly slows the graphene aggregation rate.
- (2) When two parallel graphene sheets in dodecane are in partial direct contact, they will slowly displace dodecane present between them (beyond the direct contact region) to form an aggregate. The process occurs at a constant rate since the relative sheet geometry and spacing are nearly constant in the transition region where dodecane is displaced during aggregation.
- (3) Two partially overlapped graphene sheets of equal length in close contact with one another will translate parallel to the plane of each sheet until the edges of both align and the two sheets are completely stacked. The rate of sheet realignment decreases as the overlap region between plates increases due to an increase in graphene-graphene surface areas that attract each other.

This work reveals some aspects of the behavior of graphene sheets interacting with each other in dodecane at the nanometer level. It points out relative rates of several important phenomena at near room temperature over a 25-ns time scale. Using this modeling methodology in various solvents and with varying graphene oxidation levels will increasingly provide useful insights into graphene dispersion and aggregation processes.

Acknowledgements We wish to thank the High Performance Computing Collaboratory (HPC²) at Mississippi State University for computer time.

Compliance with ethical standards

Funding This work was supported by the National Natural Science Foundation of China (grant number 51201183, 51501226) and the Fundamental Research Funds for the Central Universities (grant number 14CX02221A, 15CX08009A, and 16CX05017A).

Conflict of interest The authors declare that they have no conflict of interest.

References

- Arash B, Wang Q, Varadan VK (2014) Mechanical properties of carbon nanotube/polymer composites. *Scientific Reports* 4: 6479. doi:10.1038/srep06479
- Asche TS, Behrens P, Schneider AM (2016) Validation of the COMPASS force field for complex inorganic–organic hybrid polymers. *J Sol-Gel Sci Technol* 81:195–204. doi:10.1007/s10971-016-4185-y
- Chen S, Sun S, Li C, Pittman CU Jr, Lacy TE, Hu S, Gwaltney SR (2016) Behavior of protruding lateral plane graphene sheets in liquid dodecane: molecular dynamics simulations. *J Nanopart Res* 18:317. doi:10.1007/s11051-016-3645-1
- Eda G, Chhowalla M (2009) Graphene-based composite thin films for electronics. *Nano Lett* 9:814–818. doi:10.1021/nl8035367
- Fouquet P, Johnson MR, Hedgeland H, Jardine AP, Ellis J, Allison W (2009) Molecular dynamics simulations of the diffusion of benzene sub-monolayer films on graphite basal plane surfaces. *Carbon* 47:2627–2639. doi:10.1016/j.carbon.2009.05.018
- Geim AK, Novoselov KS (2007) The rise of graphene. *Nat Mater* 6:183–191. doi:10.1038/nmat1849
- Hu K, Kulkarni DD, Choi I, Tsukruk VV (2014) Graphene-polymer nanocomposites for structural and functional applications. *Prog Polym Sci* 39:1934–1972. doi:10.1016/j.progpolymsci.2014.03.001
- Huang X, Qi X, Boey F, Zhang H (2012) Graphene-based composites. *Nature* 41(7100):666–686. doi:10.1039/C1CS15078B
- Jang C, Lacy TE, Gwaltney SR, Toghiani H, Pittman CU Jr (2013) Interfacial shear strength of cured vinyl ester resin-graphite nanoplatelet from molecular dynamics simulations. *Polymer* 54:3282–3289. doi:10.1016/j.polymer.2013.04.035
- Jang C, Nouranian S, Lacy TE, Gwaltney SR, Toghiani H, Pittman CU Jr (2012) Molecular dynamics simulations of oxidized vapor-grown carbon nanofiber surface interactions with vinyl ester resin monomers. *Carbon* 50:748–760. doi:10.1016/j.carbon.2011.09.013
- Jiang Y, Li H, Li Y, Yu H, Liew KM, He Y, Liu X (2011) Helical encapsulation of graphene nanoribbon into carbon nanotube. *ACS Nano* 5:2026–2133. doi:10.1021/nn103317u
- Kuilla T, Bhadra S, Yao DH, Kim NH, Bose S, Lee JH (2010) Recent advances in graphene based polymer composites. *Prog Polym Sci* 35:1350–1375. doi:10.1016/j.progpolymsci.2010.07.005

- Lee C, Wei XD, Kysar JW, Hone J (2008) Measurement of the elastic properties and intrinsic strength of monolayer graphene. *Science* 321:385–388. doi:10.1126/science.1157996
- Li D, Müller MB, Gilje S, Kane RB, Wallace GG (2008) Processable aqueous dispersions of graphene nanosheets. *Nat Nanotechnol* 3:101–105. doi:10.1038/nnano.2007.451
- Li Y, Sun F, Li H (2011) Helical wrapping and insertion of graphene nanoribbon to single-walled carbon nanotube. *J Phys Chem C* 115:18459–18467. doi:10.1021/jp205210x
- Lv C, Xue Q, Xia D, Ma M, Xie J, Chen H (2010) Effect of chemisorption on the interfacial bonding characteristics of graphene–polymer composites. *J Phys Chem C* 114:6588–6594. doi:10.1021/jp100110n
- Martinez CR, Iverson BL (2012) Rethinking the term “pi-stacking”. *Chem Sci* 3:2191–2201. doi:10.1039/c2sc20045g
- Mittal G, Dhand V, Rhee KY, Park S-J, Lee WR (2015) A review on carbon nanotubes and graphene as fillers in reinforced polymer nanocomposites. *J Ind Eng Chem* 21:11–25. doi:10.1016/j.jiec.2014.03.022
- Nouranian S, Jiang C, Lacy TE, Gwaltney SR, Toghiani H, Pittman CU Jr (2011) Molecular dynamics simulations of vinyl ester resin monomer interactions with a pristine vapor-grown carbon nanofiber and their implications for composite interphase formation. *Carbon* 49:3219–3232. doi:10.1016/j.carbon.2011.03.047
- Novoselov KS, Geim AK, Morozov SV, Jiang D, Zhang Y, Dubonos SV, Grigorieva IV, Firsov AA (2004) Electric field effect in atomically thin carbon films. *Science* 306:666–669. doi:10.1126/science.1102896
- Pan F, Peng F, Jiang Z (2007) Diffusion behavior of benzene/cyclohexane molecules in poly(vinyl alcohol)-graphite hybrid membranes by molecular dynamics simulation. *Chem Eng Sci* 62:703–710. doi:10.1016/j.ces.2006.07.046
- Paton RS, Goodman JM (2009) Hydrogen bonding and π -stacking: how reliable are force fields? A critical evaluation of force field descriptions of nonbonded interactions. *J Chem Inf Model* 49:944–955. doi:10.1021/ci900009f
- Rafiee MA, Rafiee J, Srivastava I, Wang Z, Song H, Yu Z-Z, Yu N (2010) Fracture and fatigue in graphene nanocomposites. *Small* 6:179–183. doi:10.1002/smll.200901480
- Sadasivuni KK, Ponnamma D, Thomas S, Grohens Y (2014) Evolution from graphite to graphene elastomer composites. *Prog Polym Sci* 39:749–780. doi:10.1016/j.progpolymsci.2013.08.003
- Shao G, Lu Y, Wu F, Yang C, Zeng F, Wu Q (2012) Graphene oxide: the mechanisms of oxidation and exfoliation. *J Mater Sci* 47:4400–4409. doi:10.1007/s10853-012-6294-5
- Shih CJ, Lin S, Strano MS, Blankschtein D (2010) Understanding the stabilization of liquid-phase-exfoliated graphene in polar solvents: molecular dynamics simulations and kinetic theory of colloid aggregation. *J Am Chem Soc* 132:14638–14648. doi:10.1021/ja1064284
- Shokrieh MM, Shokrieh Z, Hashemianzadeh SM (2014) A novel combined molecular dynamics–micromechanics method for modeling of stiffness of graphene/epoxy nanocomposites with randomly distributed graphene. *Mater Design* 64:96–101. doi:10.1016/j.matdes.2014.07.031
- Si Y, Samulski ET (2008a) Synthesis of water soluble graphene. *Nano Lett* 8:1679–1682. doi:10.1021/nl080604h
- Si Y, Samulski ET (2008b) Exfoliated graphene separated by platinum nanoparticles. *Chem Mater* 20:6792–6797. doi:10.1021/cm801356a
- Singh V, Joung D, Zhai L, Das S, Khondaker SI, Seal S (2011) Graphene based materials: past, present and future. *Prog Mater Sci* 56:1178–1271. doi:10.1016/j.pmatsci.2011.03.003
- Stankovich S, Dikin DA, Dommett GHB, Kohlhaas KM, Zimney EJ, Stach EA, Piner RD, Nguyen ST, Ruoff RS (2006) Graphene-based composite materials. *Nature* 442:282–286. doi:10.1038/nature04969
- Sun H (1998) COMPASS: an ab initio force-field optimized for condensed-phase applications: overview with details on alkane and benzene compounds. *J Phys Chem B* 102:7338–7364. doi:10.1021/jp980939v
- Tien C-P, Teng H (2010) Polymer/graphite oxide composites as high-performance materials for electric double layer capacitors. *J Power Sources* 195:2414–2418. doi:10.1016/j.jpowsour.2009.11.001
- Wei T, Luo G, Fan Z, Zheng C, Yan J, Yao C, Li W, Zhang C (2009) Preparation of graphene nanosheet/polymer composites using in situ reduction extractive dispersion. *Carbon* 47:2290–2299. doi:10.1016/j.carbon.2009.04.030
- Wu TT, Xue QZ, Li XF, Tao YH, Jin YK, Ling CC, Lu SF (2016) Extraction of kerogen from oil shale with supercritical carbon dioxide: molecular dynamics simulations. *J of Supercritical Fluids* 107:499–506. doi:10.1016/j.supflu.2015.07.005
- Yang SY, Lin WN, Huang YL, Tien HW, Wang JY, Ma CCM, Li SML, Wang YS (2011) Synergetic effects of graphene platelets and carbon nanotubes on the mechanical and thermal properties of epoxy composites. *Carbon* 49:793–803. doi:10.1016/j.carbon.2010.10.014
- Zacharia R, Ulbricht H, Hertel T (2004) Interlayer cohesive energy of graphite from thermal desorption of polyaromatic hydrocarbons. *Phys Rev B* 69:155406. doi:10.1103/PhysRevB.69.155406
- Zhang J, Jiang D (2014) Molecular dynamics simulation of mechanical performance of graphene/graphene oxide paper based polymer composites. *Carbon* 67:784–791. doi:10.1016/j.carbon.2013.10.078
- Zhang T, Xue Q, Zhang S, Dong M (2012) Theoretical approaches to graphene and graphene-based materials. *Nano Today* 7:180–200. doi:10.1016/j.nantod.2012.04.006
- Zhao Y, Hu Z (2013) Graphene in ionic liquids: collective van der Waals interaction and hindrance of self-assembly pathway. *J Phys Chem B* 117:10540–10547. doi:10.1021/jp405660d
- Zheng QB, Xue QZ, Yan KY, Hao LZ, Li Q, Gao XL (2007) Investigation of molecular interactions between SWNT and polyethylene/polypropylene/polystyrene/polyaniline molecules. *J Phys Chem C* 111:4628–4635. doi:10.1021/jp066077c
- Zhu Y, Murali S, Cai W, Li X, Suk JW, Potts JR, Ruoff RS (2010) Graphene and graphene oxide: synthesis, properties, and applications. *Adv Mater* 22:3906–3924. doi:10.1002/adma.201001068